ACCOUNTS of chemical research

Article

pubs.acs.org/accounts

Single-Molecule Imaging of Dynamic Motions of Biomolecules in DNA Origami Nanostructures Using High-Speed Atomic Force Microscopy

Masayuki Endo*[,†,§] and Hiroshi Sugiyama*[,†,‡,§]

[†]Institute for Integrated Cell-Material Sciences (WPI-iCeMS), Kyoto University, Yoshida-ushinomiyacho, Sakyo-ku, Kyoto 606-8501, Japan

[‡]Department of Chemistry, Graduate School of Science, Kyoto University, Kitashirakawa-oiwakecho, Sakyo-ku, Kyoto 606-8502, Japan

[§]CREST, Japan Science and Technology Corporation (JST), Sanbancho, Chiyoda-ku, Tokyo 102-0075, Japan

CONSPECTUS: Direct imaging of molecular motions is one of the most fundamental issues for elucidating the physical properties of individual molecules and their reaction mechanisms. Atomic force microscopy (AFM) enables direct molecular imaging, especially for biomolecules in the physiological environment. Because AFM can visualize the molecules at nanometer-scale spatial resolution, a versatile observation scaffold is needed for the precise imaging of molecule interactions in the reactions.

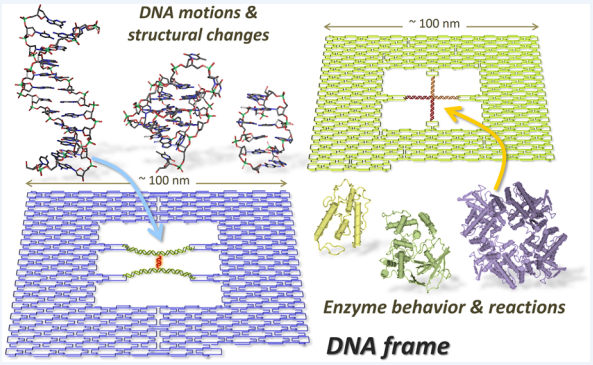

The emergence of DNA origami technology allows the precise placement of desired molecules in the designed nanostructures and enables molecules to be detected at the single-molecule level. In our study, the DNA origami system was applied to visualize the detailed motions of target molecules in reactions using high-speed AFM (HS-AFM), which enables the analysis of dynamic motions of biomolecules in a subsecond time resolution. In this system, biochemical properties such as the placement of various double-stranded DNAs (dsDNAs) containing unrestricted DNA sequences, modified nucleosides, and chemical functions can be incorporated. From a physical point of view, the tension and rotation of dsDNAs can be controlled by placement into the DNA nanostructures. From a topological point of view, the orientations of dsDNAs and various shapes of dsDNAs including Holliday junctions can be incorporated for studies on reaction mechanisms.

In this Account, we describe the combination of the DNA origami system and HS-AFM for imaging various biochemical reactions including enzymatic reactions and DNA structural changes. To observe the behaviors and reactions of DNA methyltransferase and DNA repair enzymes, the substrate dsDNAs were incorporated into the cavity of the DNA frame, and the enzymes that bound to the target dsDNA were observed using HS-AFM. DNA recombination was also observed using the recombination substrates and Holliday junction intermediates placed in the DNA frame, and the direction of the reactions was controlled by introducing structural stress to the substrates. In addition, the movement of RNA polymerase and its reaction were visualized using a template dsDNA attached to the origami structure. To observe DNA structural changes, G-quadruplex formation and disruption, the switching behaviors of photoresponsive oligonucleotides, and B−Z transition were visualized using the DNA frame observation system. For the formation and disruption of G-quadruplex and double-helix DNA, the two dsDNA chains incorporated into the DNA frame could amplify the small structural change to the global structural change, which enabled the visualization of their association and dissociation by HS-AFM. The dynamic motion of the helical rotation induced by the B−Z transition was also directly imaged in the DNA frame. Furthermore, the stepwise motions of mobile DNA along the DNA track were visualized on the DNA origami surface. These target-orientated observation systems should contribute to the detailed analysis of biomolecule motions in real time and at molecular resolution.

1. INTRODUCTION

Live imaging of target biomolecules is one of the goals for scientists wishing to study various phenomena involved in living systems and for investigations into the physical properties of molecules. Direct imaging using a probe microscope is a practical approach for investigating the motions of biomolecules during reactions. Atomic force microscopy (AFM) enables the direct observation of biomolecules at nanoscale spatial resolution, and the imaging can be performed under physiological conditions. To facilitate the observation of single

Special Issue: Nucleic Acid Nanotechnology

Received: December 13, 2013
Published: March 6, 2014

ACS Publications © 2014 American Chemical Society

biomolecules, a versatile observation scaffold is needed for the precise analysis of interactions and reactions.[1,2] DNA origami,[3] a new DNA self-assembly system based on well-established DNA nanotechnology, has recently been developed for the construction of a wide variety of multidimensional nanostructures. These can be used as scaffolds for incorporation of various functionalities at desired positions. The DNA origami system is expanded for single-molecule detection of target molecules and for the analysis of single chemical reactions, which are imaged by AFM.[1,2] The various states of individual molecules can be imaged on the DNA origami surface when using the DNA nanostructure as a scaffold for AFM observation. Therefore, the detailed dynamics of the molecules can also be visualized if the single-molecule imaging is performed on the DNA origami structure. In the past decade, high-speed AFM (HS-AFM) has enabled the visualization of molecular movement during biological reactions in a subsecond time scale.[4−7] To enable high-speed imaging, a small cantilever with a high resonance frequency (0.6−1.2 MHz in water) and small spring constant (0.1−0.2 N/m) was developed, and a high-speed scanner was also developed to prevent resonant vibrations during scanning.[4−9] These improvements realized a 5−20 frames/s imaging rate (depending on the scanning dimension and the number of data points), which enabled the dynamic motions of biomolecules to be imaged in real time at molecular resolution.[4−9] With the DNA origami system and HS-AFM, the dynamic movement of mobile molecules can be imaged when the substrate double-stranded DNA (dsDNA) is attached to the robust origami structure. The DNA origami system is expected to be expanded to image the dynamic movement of various biomolecules, including enzymatic reactions and DNA structural changes at the single-molecule level.[1,10]

2. DIRECT SINGLE-MOLECULE OBSERVATION OF ENZYMES IN THE DNA NANOSTRUCTURE

To directly observe the dynamic motions of the enzymes interacting with a substrate dsDNA, several studies have been performed using HS-AFM.[11−13] In these studies, it is difficult to obtain a homogeneous dsDNA substrate because the dsDNA forms various random shapes. To overcome this problem, we created an observation scaffold based on the DNA origami structure carrying substrate dsDNAs. We designed and prepared a DNA origami scaffold called a "DNA frame", which looks like a nanoscale photo frame, for this purpose. This robust DNA frame can accommodate two different dsDNA fragments in its cavity (ca. 40 nm × 40 nm) to control physical properties such as the tensions of incorporated dsDNAs (Figure 1A).[10]

2.1. DNA Methyltransferase

DNA-modifying enzymes often require the bending of specific DNA strands to facilitate reactions. DNA methylation enzyme *Eco*RI methyltransferase (M.*Eco*RI) bends dsDNA by 55−59°, enabling the methyl-transfer reaction to proceed.[14] To examine the DNA bending effect on methylation with M.*Eco*RI, two different lengths of dsDNA fragments, 64 bp and 74 bp dsDNA, were incorporated into the DNA frame structure.[10] Because the length between connectors in the DNA frame cavity is 64 bp, 64 bp dsDNA fits to the DNA frame as a tense form in which its conformational flexibility should be suppressed, while the 74 bp dsDNA is more relaxed, allowing local dsDNA bending. The dynamic movements of the

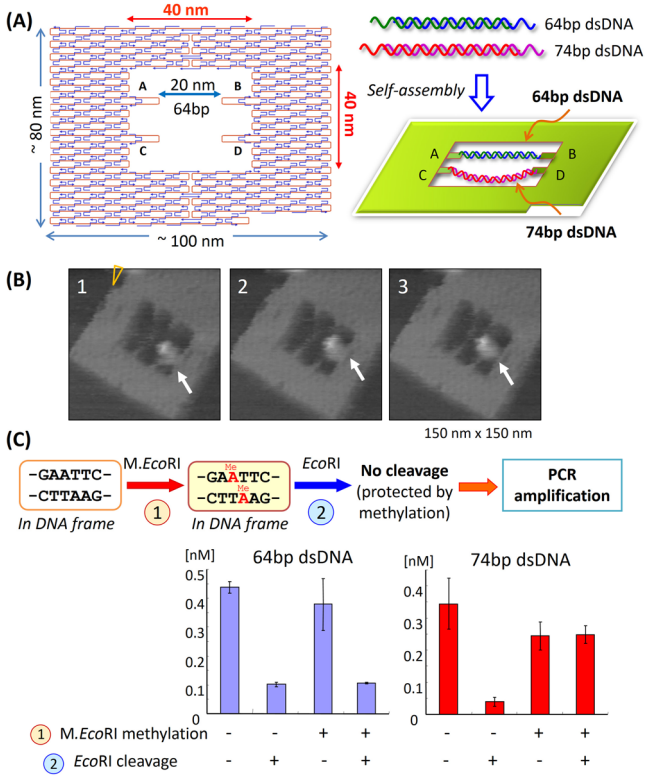

Figure 1. Regulation of the methylation reactions of M.*Eco*RI in the DNA origami scaffold and HS-AFM images of M.*Eco*RI movement. (A) DNA frame structure designed to incorporate two different dsDNAs, tense 64 bp dsDNA and relaxed 74 bp dsDNA, which contain a specific sequence for M.*Eco*RI at the center. (B) HS-AFM images of M.*Eco*RI moving on the 64 bp dsDNA in the DNA frame. Successive AFM images were taken at a scanning rate of 1.0 frame/s. (C) Quantification of DNA methylation in the DNA frame. When methylation occurs, the target sequence is protected from subsequent cleavage by restriction enzyme *Eco*RI, resulting in amplification of the target sequence by PCR. The graphs show the quantification of methylation of the target site in 64 bp and 74 bp dsDNA by real-time PCR amplification.

dsDNAs and the formation of M.*Eco*RI complexes with dsDNAs were observed by HS-AFM (Figure 1B). After treatment of the dsDNA in the DNA frame with M.*Eco*RI and subsequent digestion with restriction enzyme *Eco*RI, AFM analysis revealed that the 74 bp dsDNA was less effectively cleaved compared with the 64mer dsDNA. This indicates that the methylation occurred preferentially in the relaxed 74 bp dsDNA rather than in the tense 64 bp dsDNA. Biochemical analysis of the methylation to the target sequence was performed using real-time polymerase chain reaction (PCR). After methylation with M.*Eco*RI and subsequent *Eco*RI digestion, the 74 bp dsDNA substrate in the DNA frame was efficiently amplified, indicating the preferential methylation to the target sequence in the 74 bp dsDNA (Figure 1C). These results show the importance of structural flexibility for the bending of dsDNA during the methyl-transfer reaction with M.*Eco*RI. Therefore, DNA methylation can be regulated using the tension-controlled dsDNAs created in the DNA frame.

2.2. DNA Base-Excision Repair Enzymes

DNA repair is an indispensable biological function to preserve genetic information from mutations such as transversion during replication.[15] DNA base-excision repair enzymes 8-oxoguanine

dx.doi.org/10.1021/ar400299m | *Acc. Chem. Res.* 2014, 47, 1645−1653

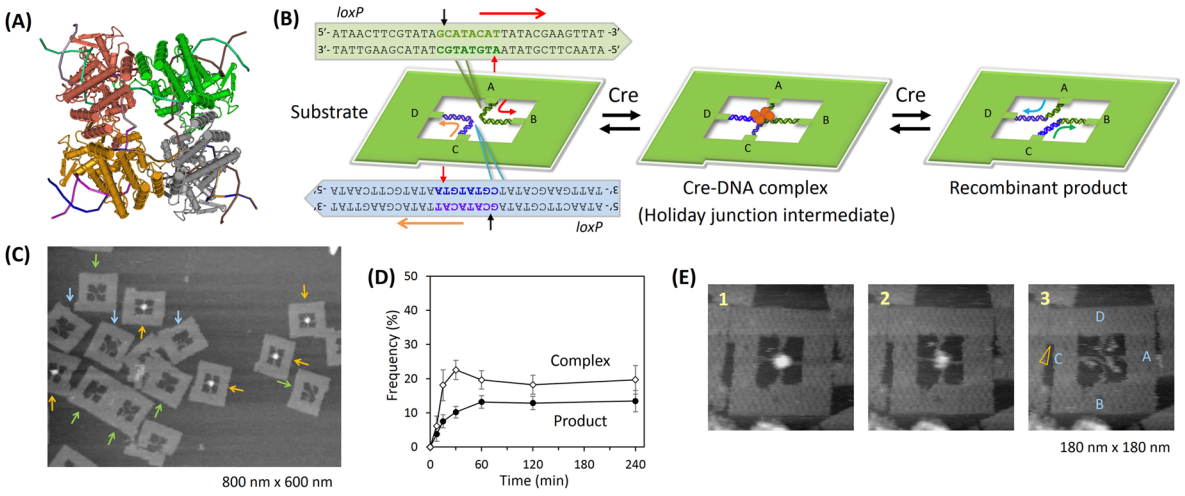

Figure 2. Regulation and single-molecule observation of Cre-mediated recombination in the DNA frame. (A) Crystal structure of the Cre tetramer bound to the Holliday junction intermediate (PDB 3CRX). (B) Substrate dsDNAs containing the *lox*P sequence in the antiparallel orientation were placed in the DNA frame. In the recombination, the Cre tetramer forms a synaptic complex and subsequently generates a recombinant product, which is easily identified by the topological arrangement of two dsDNAs as different loop structures and a cross-shape. (C) AFM image of the substrate in the DNA frame after incubation with Cre. The Cre−DNA complex, starting substrate, and recombinant product are indicated by orange, green, and blue arrows, respectively. (D) Time-course analysis of the formation of the Cre−DNA complex and recombinant product. (E) HS-AFM images of the dissociation of the Cre tetramer from the dsDNAs into four Cre monomers and the appearance of a recombinant product. Successive AFM images were taken at a scanning rate of 1.0 frame/s.

glycosylase (hOgg1) and T4 pyrimidine dimer glycosylase (PDG) were employed for the analysis of reactions on the DNA nanostructure.[16] These enzymes have glycosylase/AP lyase activity, which removes damaged nucleobases and cleaves the DNA strand. Repair enzymes often require local structural changes in the target DNA strands, such as DNA bending, for the reaction to proceed.[17,18] hOgg1 bends dsDNA about 70° to flip out the oxoG base so that the reaction proceeds.[19] PDG also bends the double helix by 60° to flip out the 3′-side of adenine in the opposite strand of the thymine dimer.[20,21] Various dsDNAs containing a damaged base were incorporated into the DNA frame as dsDNA cassettes, and the repair reactions were analyzed at the single-molecule level. To examine the structural effect on glycosylase/AP lyase activity including cleavage of the DNA strand and the trapping of reaction intermediates, two different lengths of substrate dsDNAs, tense 64 bp and relaxed 74 bp dsDNAs, were placed into the DNA frame. The enzymes more favorably cleaved the relaxed dsDNA and were covalently trapped after $NaBH_4$ reduction compared with the tense dsDNA. In addition, enzyme movement and the DNA repair reaction were directly observed on the DNA frame using HS-AFM. The DNA frame system serves to analyze the detailed repair process by directly observing the events involved in DNA repair such as binding, sliding, catalytic reaction, and dissociation.

2.3. DNA Recombinase

DNA recombination plays important roles, including the generation of genetic diversity and mediating DNA integration into the host genome.[22] Cre recombinase recognizes the 34 bp *lox*P sequence and forms a synaptic complex with two *lox*P dsDNAs as a tetramer form.[23,24] Here, substrate dsDNAs with the *lox*P sequence were placed in a DNA scaffold, and the recombination events were analyzed at the single-molecule level (Figure 2).[25]

The DNA frame can control the orientation of two *lox*P sequences in antiparallel and parallel arrangements. First, recombination was directly observed using the dsDNA substrates in antiparallel arrangement in the DNA frame (Figure 2B). Cre performs two-step cleavage/strand exchange reactions to form the Holliday junction (HJ) intermediate and recombinant product. After incubation with Cre, the Cre−DNA complex and recombinant products were clearly observed in the DNA frame, showing that recombination occurred using the substrates placed in the nanospace (Figure 2C). Over the reaction time course, the Cre−DNA complex formed first, followed by the recombinant product (Figure 2D). During observation of the Cre−DNA complex by HS-AFM, the tetrameric Cre that formed the synaptic complex dissociated into four monomers, and the recombinant product simultaneously appeared (Figure 2E). In the parallel arrangement, the Cre−DNA complex was formed, while the recombinant product was not observed.

The DNA scaffold can also control the angle of the HJ and impose structural stress. To regulate the direction of recombination, the HJ intermediates crossing at 90° and 60° were prepared using different DNA frames.[25] By adjusting the directions of the *lox*P sequences, the HJ intermediates crossing at 90° were resolved to give products in the usual way.[26,27] On the other hand, the reaction with HJ intermediates crossing at 60° changed the formation of the resolution products by different proportions. Therefore, the structural stress imposed on the HJ intermediates in the DNA frames can regulate the direction of recombination. The desired geometric arrangements of the substrate dsDNAs using the DNA frames are valuable for studying recombination events, which are effectively controlled by the orientation of substrate dsDNAs and the angle of HJ intermediates.

We have also successfully visualized transcription including sliding of T7 RNA polymerase and RNA synthesis using a template dsDNA-attached nanoscaffold and HS-AFM.[28] The observation system can be used for a wide variety of DNA-binding proteins and enzymes that move along dsDNA during the reaction. A combination of the DNA origami nanoscaffold and HS-AFM is an intelligent system for observing enzymatic

dx.doi.org/10.1021/ar400299m | *Acc. Chem. Res.* 2014, 47, 1645−1653

reactions and relevant events including complex formation, catalysis, and dissociation at the single-molecule resolution.

3. DIRECT IMAGING OF DNA STRUCTURAL CHANGES IN THE DNA ORIGAMI STRUCTURE

Structural variations and conformational changes in the DNA involved in living systems are closely linked to the regulation of their biological functions, such as gene expression.[29,30] The DNA frame system allows the introduction of various dsDNAs with unrestricted sequences for observation of reactions, and DNA frames can also control the physical properties of dsDNAs such as the tensions and rotations of double-helices. Here, the DNA frame system is applied for the visualization of DNA structural changes involved in the formation and disruption of the G-quadruplex and photoresponsive duplex and helical rotation in the B–Z transition.

3.1. G-Quadruplex Formation and Disruption

In the field of structural and molecular biology, G-quadruplex, a four-stranded helix structure, is of great interest because of its structural variations and biological functions.[31] For the detection of the formation and disruption of a G-quadruplex structure, we employed our observation system by monitoring the shape of dsDNA chains in the DNA frame.[32] Two dsDNA chains containing single-stranded triple guanine (GGG) overhangs at the center were prepared for the interstrand G-quadruplex formation.[33] Three G-tracts were placed in the upper dsDNA chain, whereas the lower dsDNA chain had a single G-tract (Figure 3A). Initially, the two dsDNA chains

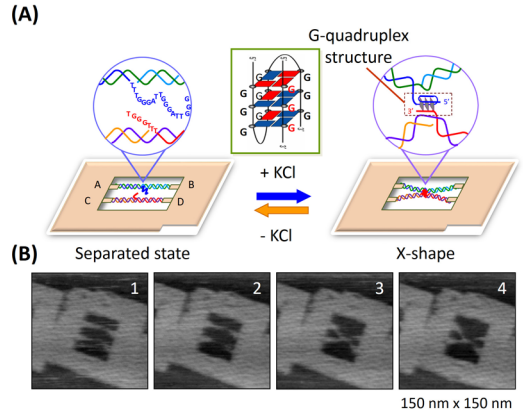

Figure 3. Visualization of G-quadruplex formation using the structural change of two dsDNA chains placed in the DNA frame. (A) In the presence of KCl, the separated state changes to the X-shape by connection at the center of two dsDNA chains via G-quadruplex formation. (B) HS-AFM images for the formation of an X-shape structure by the association of two dsDNA chains via G-quadruplex formation. Four successive AFM images were taken at a scanning rate of 0.2 frames/s.

introduced did not contact each other. In the presence of K^+, the two dsDNA chains in the DNA frame clearly showed an X-shaped structure with a 44% yield, demonstrating the formation of an interstrand G-quadruplex. The dynamic formation of the G-quadruplex was further examined in real time by HS-AFM. During scanning of the sample in the presence of K^+, the two dsDNA chains with G-tracks maintained a separated state for a given period, and then they suddenly formed the X-shaped structure (Figure 3B). In a similar fashion, the disruption of the preformed G-quadruplex was directly observed in the absence of K^+. The X-shape remained unchanged for a while, and then it reverted to the separated state during AFM scanning.

Furthermore, four DNA strands containing various G-tracts were assembled in the DNA frame to form a synaptic G-quadruplex using the same system.[34,35] Thus, the single-molecule observation of the dynamic formation and disruption of a G-quadruplex was successfully achieved by monitoring the global structural changes of the two incorporated dsDNA chains in the DNA frame using HS-AFM.

3.2. Hybridization and Dissociation of Photoresponsive Oligonucleotides

The direct observation of hybridization and dissociation of a double-helix DNA at molecular resolution is quite challenging. The dynamic hybridization and dissociation of DNA strands were examined on the DNA origami scaffold using fluorescence microscopy by tracking fluorescence-labeled DNA strands.[36] AFM-based single-molecule imaging can visualize whole nanostructures by directly monitoring the shape of DNA strands. Photoresponsive oligonucleotides (ODNs) containing azobenzene moieties were employed to observe the hybridization and dissociation of duplex DNA.[37,38] A pair of photoresponsive ODNs was connected to the individual dsDNA chains, which were then placed in the cavity of the DNA frame (Figure 4A).[39] The photoresponsive domain can hybridize with the corresponding counterpart in the *trans*-form of the azobenzene moiety and dissociate in the *cis*-form under ultraviolet (UV) irradiation.[38] The dissociated ODNs in the *cis*-form hybridize again upon visible light (vis) irradiation.[38] Two dsDNA chains possessing photoresponsive domains at the center were placed in the cavity of the DNA frame. The hybridized photoresponsive duplex in the center of the dsDNA chains in the DNA frame was clearly visualized (Figure 4B). Using this origami system, hybridization and dissociation can be identified by the global structural change of the two dsDNA chains as an X-shape and as a separated shape in the DNA frame, respectively. Hybridization and dissociation were observed directly using HS-AFM. The dissociation of the two dsDNA chains in contact at the center (X-shape) was imaged during UV irradiation. The contact of the two separated dsDNA chains in the center was then imaged again during vis irradiation (Figure 4C). Successive switching of dissociation and hybridization of the photoresponsive domains was visualized at the single-molecule level by observing the global change of two dsDNA chains, the X-shape and the separated shape, in the DNA frame.

3.3. B–Z Transition in the Equilibrium State

A right-handed B-form dsDNA containing the CG repeat sequence is known to transit to the left-handed Z-form structure when the salt concentration is increased.[40] A nanomechanical device employing the rotation of the B–Z transition was created on the DNA nanostructure, and the rotation of the nanostructure was investigated by FRET.[41] In our observation system, a rotary motion of double-helix DNA during the B–Z conformational transition was directly visualized in the DNA frame structure.[42] To visualize the B–Z transition, a dsDNA with a 5-methyl-CG six-repeat sequence $(^{me}CG)_6$ and a flag marker containing three bundled dsDNAs connected by crossovers was introduced to the DNA frame (Figure 5). The $(^{me}CG)_6$ repeat can promote the formation of a Z-form even at low salt concentrations.[43] One dsDNA with a $(^{me}CG)_6$ sequence and the flag was introduced to the top as a B–Z transition system, and the other dsDNA with a random

dx.doi.org/10.1021/ar400299m | *Acc. Chem. Res.* 2014, 47, 1645–1653

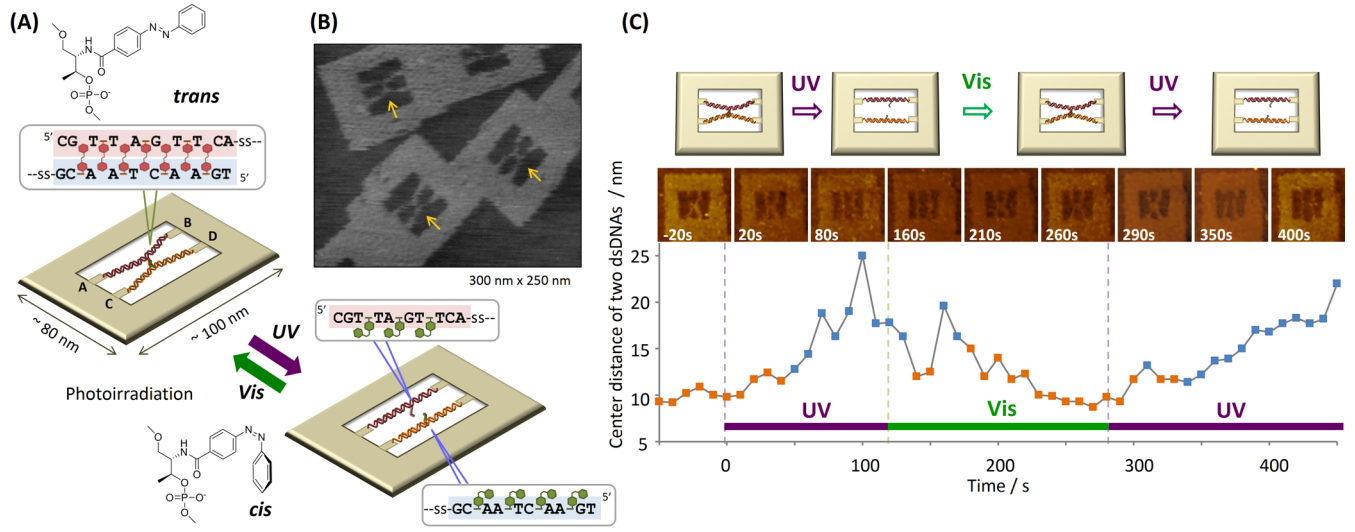

Figure 4. Direct observation of the hybridization and dissociation of a pair of photoresponsive ODNs. (A) Single-molecule observation system constructed in the DNA frame. In the *trans*-form of an azobenzene moiety, two photoresponsive domains hybridize to form a duplex. In the *cis*-form induced by UV irradiation, the two domains dissociate. Two dsDNA chains containing photoresponsive ODNs were placed in the DNA frame to observe the dissociation and hybridization after UV and vis irradiation, respectively. Two different dsDNA chains containing different photoresponsive ODNs were connected between the specific connection sites in the DNA frame via the corresponding overhanging ssDNAs. (B) AFM image of the photoresponsive duplex supported by two dsDNA chains in the DNA frame (orange arrow). (C) Photoswitching activity of photoresponsive ODNs in the DNA frame. The repeating dissociation and hybridization was visualized by HS-AFM during alternative UV/vis photoirradiation. The distance between the centers of two dsDNA chains was plotted. The appearance of an X-shape and a separated shape is shown as an orange and blue rectangle in the graph, respectively.

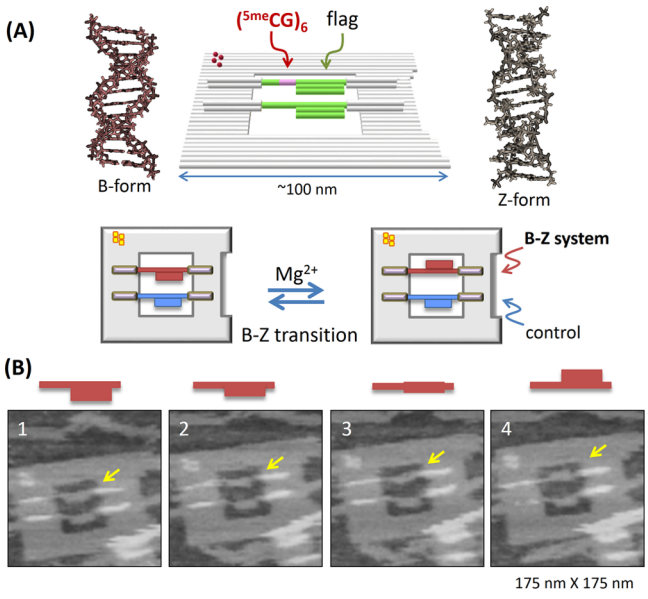

Figure 5. Direct observation of B−Z transition in the DNA frame. (A) B- and Z-form dsDNA structures and single-molecule observation system for B−Z transition. Two dsDNAs having a $(^{5me}CG)_6$ sequence (B−Z system) and a random sequence (control) were introduced to the top and bottom site in the DNA frame, respectively. For observation of the dsDNA rotation, both of the ssDNA linkers in the left terminus of the dsDNA were fixed to the connector, while one ssDNA linker in the right terminus was attached to the connector. The dsDNAs have a flag marker for observation of the rotation of the dsDNA shaft during B−Z transition. (B) HS-AFM images of the flipping motion of the flag marker at the top site (yellow arrow). Four successive images are presented at a scanning rate of 0.2 frames/s.

sequence and the flag was introduced to the bottom as a control. To allow rotation during the B−Z transition, four connectors in the DNA frame were designed to lift the dsDNAs from the scaffold surface (Figure 5A). In addition, for observation of the rotation of double-helix, both of the single-stranded DNA (ssDNA) linkers in the left terminus of the dsDNA were fixed to the connector, while one ssDNA linker in the right terminus was attached to the connector. When the B−Z transition occurs, the flag marker rotates around the dsDNA shaft, and the rotary motion should be observed by monitoring the position of the flag. Upon increase of the concentration of Mg ions, the proportion of the flag marker of the B−Z system rotated to the upper side increased to 70%, whereas 76% of the flag in the control remained unchanged. Further, by control of the concentration of Mg ions, the rotation of the flag marker of the B−Z system was imaged directly by HS-AFM under equilibrium conditions for the B−Z transition state. The flag movement of the B−Z system was observed during AFM scanning (Figure 5B). The successive images also show the height change of the flag, indicating the rotation of the flag marker around the dsDNA shaft containing the B−Z transition system.

With the DNA origami scaffold and HS-AFM system, important DNA conformational changes including G-quadruplex formation and B−Z transition were successfully imaged. In addition, the dissociation and hybridization of photoresponsive DNAs, which were precisely controlled by photoirradiation using different wavelengths, were directly visualized in the origami structure. The observation system in these experiments can be used as a general strategy for investigating various DNA structural changes and molecular switches working as a single molecule. It can also be applied to the single-molecule imaging of chemical reactions such as bond formation and cleavage.

dx.doi.org/10.1021/ar400299m | *Acc. Chem. Res.* 2014, 47, 1645−1653

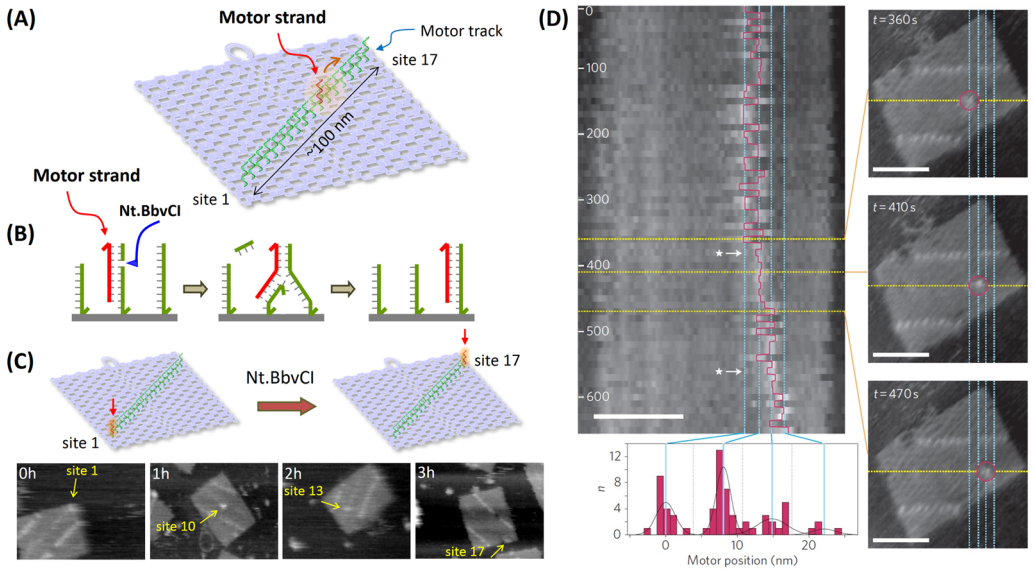

Figure 6. Direct observation of DNA motor movement on the DNA origami surface. (A) A motor track consisting of 17 stators (green ssDNAs) was constructed on the DNA origami surface, and the movement of the DNA motor (red ssDNA) was examined. (B) Mechanism of the DNA motor movement. When a stator ssDNA (green ssDNA), which forms a duplex with a DNA motor (red ssDNA), is cleaved by the nicking enzyme Nt.BbvCI, the motor strand moves to the adjacent stator strand by branch migration. (C) AFM images of time-dependent movement of a DNA motor. A duplex containing a DNA motor strand was visualized as a white dot. (D) Stepwise movement of a DNA motor observed by HS-AFM, and a kymograph and distribution of the motor positions. Scale bar 50 nm.

4. DIRECT OBSERVATION OF A MOBILE DNA NANOMACHINE MOVING ALONG THE TRACK ON THE DNA ORIGAMI SURFACE

Considering the programmability of DNA sequences and the manipulation of association and dissociation of duplexes, DNA has been used for various molecular machines.[44] DNA nanomachines such as DNA tweezers and various walking devices have been developed by manipulating duplex formation using strand displacement.[44]

A DNA transportation system was constructed with a mobile DNA nanomachine moving along a designed track on the DNA origami surface (Figure 6A). The track on the DNA scaffold was constructed to observe the multistep movement of a specific DNA strand.[45] Multiple ssDNAs (stators) were introduced onto the rectangular DNA origami tile as a track to hybridize a complementary mobile DNA strand (motor strand). As shown in Figure 6B, when a DNA motor strand hybridizes to the specific stator strand, the stator/motor duplex is subsequently cleaved by the nicking enzyme Nt.BbvCI, which removes the short ssDNA from the stator.[46] The motor strand then binds to the neighboring intact stator by branch migration and finally moves forward. The DNA tile carrying the motor strand at the initial position was incubated with Nt.BbvCI to examine the migration of the motor strand along the DNA motor track. The motor strand was imaged as a single spot of the duplex on the DNA origami scaffold, which was easily distinguished from the invisible single-stranded stators. Time-dependent movement of the motor strand along the motor track was observed (Figure 6C). Furthermore, the movement of the motor strand was directly visualized by HS-AFM. The stator/motor duplex spot showed back and forth movement along the motor track and finally moved forward during AFM scanning. From the kymograph analysis, the distance of the motor-strand movement corresponded to the distance between the adjacent stators, indicating that the movement occurred stepwise on the track (Figure 6D).

A programmed DNA motor system was constructed using the predesigned DNA track on the DNA origami scaffold. By employing HS-AFM, the detailed motion of the DNA motor was directly observed and analyzed. The method was further applied to regulate the transportation of a DNA motor on a branched motor track, where the direction of the movement of the DNA motor was precisely controlled by specifically blocking and releasing strands with predefined instructions.[47] Related works, such as a DNA spider[48] and a programmed assembly line,[49] which also used a mobile DNA nanomachine and DNA origami scaffold, have been reported for the construction of a nanoscale transportation system.

5. LIMITATIONS OF AFM IMAGING AND COMPARISON WITH OTHER IMAGING TECHNIQUES

Although AFM imaging can be performed at high spatial resolution, one of the drawbacks in dynamic measurement is the interaction with the mica surface. This should always be considered as an experimental artifact in the measurement of the dynamic movement of molecules. To reduce the unwanted interaction with the surface during high-speed scanning, lipid bilayers and streptavidin crystal layers are used to coat the mica surface.[50,51] The origami surface could be used to prevent the direct contact of molecules on the surface, as achieved in the DNA motor experiment. Tip−sample interaction forces in AFM analysis are an unavoidable problem, and the target complex is sometimes broken during multiple scanning. For the non-invasive scanning, feedback controller to regulate the cantilever oscillation amplitude was improved to reduce the tip-sample interaction.[52] This strategy can improve the maintenance of complexes. For example, the translocation of myosin V molecules along actin filaments was imaged without damage during multiple scanning in a high-speed mode.[53] Methods to reduce damage to biomolecule samples are now being developed.[6]

dx.doi.org/10.1021/ar400299m | Acc. Chem. Res. 2014, 47, 1645−1653

Recently, the super-resolution total-internal-reflection fluorescence microscope, which can monitor the position of a fluorescent molecule on the DNA origami surface, has been employed to track target molecules.[36,54−59] With this method, the consecutive movement of a DNA spider on a track constructed on a DNA origami tile was monitored in real time.[48] The dynamic hybridization and dissociation of dsDNA was also monitored on a DNA origami structure.[36] Fluorescence imaging is advantageous for tracking labeled target molecules in real time, but detailed information on morphological changes of whole nanostructures cannot be imaged simultaneously. Both AFM and fluorescence imaging techniques could be employed to compensate for individual weak points.

6. CONCLUSIONS AND PERSPECTIVES

DNA origami technology allows the construction of a desired nanostructure and the precise placement and manipulation of target molecules. In these studies, the designed nanospace has been used to observed and regulate enzymatic reactions and DNA structural changes. Using the advantageous features of DNA origami technology, single-molecule observation systems have been developed by creating target-oriented nanospaces and introducing target dsDNAs for desired observations. The method we have developed can be expanded to the analysis and regulation of various biochemical reactions involved in gene expression and other biological phenomena such as replication, transcription, and translation. Single chemical reactions such as complex formations, photoreactions, and bond formation/cleavage can also be imaged using this system. The HS-AFM observation of DNA origami has now been performed on a lipid bilayer,[51] so that the undesired interaction between a target molecule and mica surface should be avoided during AFM scanning. In addition, the movement of artificial mobile molecules has been directly observed and manipulated in the designed DNA origami system, and the detailed mechanism for the motion of the molecules has been investigated at the single-molecule level. To understand the working principle of the biological system, the single-molecule observation system created in the designed nanostructure can be applied for the detailed analysis of multistep biological reactions simultaneously and sequentially at molecular resolution.

AUTHOR INFORMATION

Corresponding Authors

*E-mail: endo@kuchem.kyoto-u.ac.jp (M.E.)
*E-mail: hs@kuchem.kyoto-u.ac.jp (H.S.).

Funding

The authors are financially supported by Core Research for Evolutional Science and Technology (CREST) of JST and JSPS KAKENHI (Grant Numbers 24310097, 24104002, and 25253004).

Notes

The authors declare no competing financial interest.

Biographies

Masayuki Endo graduated from Kyoto University (Prof. I. Saito) and received his Ph.D. at the University of Tokyo (Prof. M. Komiyama) in 1997. He moved to Tokyo Medical and Dental University (Prof. H. Sugiyama) as a JSPS Postdoctoral fellow. He continued research in the Verdine group at Harvard University as a CRI Postdoctoral fellow (1998−2000). After working in the Yokoyama group at RIKEN, he joined Osaka University as an Assistant Professor (2001−2008). During that time in 2005, he had an opportunity to carry out the research in the Seeman group (New York University) as a visiting scholar. Since 2008, he has been in Institute for Integrated Cell-Material Sciences (WPI-iCeMS), Kyoto University, as an Associate Professor. His work involves DNA chemical biology and DNA nanotechnology.

Hiroshi Sugiyama received his Ph.D. in 1984 with Teruo Matuura at Kyoto University. After postdoctoral studies at the University of Virginia with Sidney M. Hecht, he returned to Kyoto University in 1986 as an Assistant Professor and became an Associate Professor in 1993. In 1996, he joined the Institute of Biomaterials and Bioengineering at Tokyo Medical and Dental University. He has been a Professor of Chemical Biology at Kyoto University since 2003. Among the honors he has received are the Nippon IBM Award and the Chemical Society of Japan Award for Creative Work.

REFERENCES

(1) Rajendran, A.; Endo, M.; Sugiyama, H. Single-molecule analysis using DNA origami. *Angew. Chem., Int. Ed.* **2012**, *51*, 874−890.
(2) Torring, T.; Voigt, N. V.; Nangreave, J.; Yan, H.; Gothelf, K. V. DNA origami: A quantum leap for self-assembly of complex structures. *Chem. Soc. Rev.* **2011**, *40*, 5636−5646.
(3) Rothemund, P. W. Folding DNA to create nanoscale shapes and patterns. *Nature* **2006**, *440*, 297−302.
(4) Ando, T.; Kodera, N.; Takai, E.; Maruyama, D.; Saito, K.; Toda, A. A high-speed atomic force microscope for studying biological macromolecules. *Proc. Natl. Acad. Sci. U.S.A.* **2001**, *98*, 12468−12472.
(5) Ando, T.; Uchihashi, T.; Kodera, N. High-Speed AFM and Applications to Biomolecular Systems. *Annu. Rev. Biophys.* **2013**, *42*, 393−414.
(6) Uchihashi, T.; Kodera, N.; Ando, T. Guide to video recording of structure dynamics and dynamic processes of proteins by high-speed atomic force microscopy. *Nat. Protoc.* **2012**, *7*, 1193−1206.
(7) Rajendran, A.; Endo, M.; Sugiyama, H. State-of-the-art high-speed atomic force microscopy for investigation of single-molecular dynamics of proteins. *Chem. Rev.* **2014**, *114*, 1493−1520.
(8) Walters, D. A.; Cleveland, J. P.; Thomson, N. H.; Hansma, P. K.; Wendman, M. A.; Gurley, G.; Elings, V. Short cantilevers for atomic force microscopy. *Rev. Sci. Instrum.* **1996**, *67*, 3583−3590.
(9) Schitter, G.; Astrom, K. J.; DeMartini, B. E.; Thurner, P. J.; Turner, K. L.; Hansma, P. K. Design and modeling of a high-speed AFM-scanner. *Ieee T. Contr. Syst. T.* **2007**, *15*, 906−915.
(10) Endo, M.; Katsuda, Y.; Hidaka, K.; Sugiyama, H. Regulation of DNA methylation using different tensions of double strands constructed in a defined DNA nanostructure. *J. Am. Chem. Soc.* **2010**, *132*, 1592−1597.
(11) Crampton, N.; Yokokawa, M.; Dryden, D. T.; Edwardson, J. M.; Rao, D. N.; Takeyasu, K.; Yoshimura, S. H.; Henderson, R. M. Fast-scan atomic force microscopy reveals that the type III restriction enzyme EcoP15I is capable of DNA translocation and looping. *Proc. Natl. Acad. Sci. U.S.A.* **2007**, *104*, 12755−12760.
(12) Gilmore, J. L.; Suzuki, Y.; Tamulaitis, G.; Siksnys, V.; Takeyasu, K.; Lyubchenko, Y. L. Single-molecule dynamics of the DNA−*Eco*RII protein complexes revealed with high-speed atomic force microscopy. *Biochemistry* **2009**, *48*, 10492−10498.
(13) Suzuki, Y.; Gilmore, J. L.; Yoshimura, S. H.; Henderson, R. M.; Lyubchenko, Y. L.; Takeyasu, K. Visual analysis of concerted cleavage by type IIF restriction enzyme SfiI in subsecond time region. *Biophys. J.* **2011**, *101*, 2992−2998.
(14) Youngblood, B.; Reich, N. O. Conformational transitions as determinants of specificity for the DNA methyltransferase EcoRI. *J. Biol. Chem.* **2006**, *281*, 26821−26831.
(15) David, S. S.; O'Shea, V. L.; Kundu, S. Base-excision repair of oxidative DNA damage. *Nature* **2007**, *447*, 941−950.

(16) Endo, M.; Katsuda, Y.; Hidaka, K.; Sugiyama, H. A versatile DNA nanochip for direct analysis of DNA base-excision repair. *Angew. Chem., Int. Ed.* **2010**, *49*, 9412−9416.
(17) Nash, H. M.; Bruner, S. D.; Scharer, O. D.; Kawate, T.; Addona, T. A.; Spooner, E.; Lane, W. S.; Verdine, G. L. Cloning of a yeast 8-oxoguanine DNA glycosylase reveals the existence of a base-excision DNA-repair protein superfamily. *Curr. Biol.* **1996**, *6*, 968−980.
(18) Vassylyev, D. G.; Morikawa, K. DNA-repair enzymes. *Curr. Opin. Struct. Biol.* **1997**, *7*, 103−109.
(19) Bruner, S. D.; Norman, D. P.; Verdine, G. L. Structural basis for recognition and repair of the endogenous mutagen 8-oxoguanine in DNA. *Nature* **2000**, *403*, 859−866.
(20) Morikawa, K.; Matsumoto, O.; Tsujimoto, M.; Katayanagi, K.; Ariyoshi, M.; Doi, T.; Ikehara, M.; Inaoka, T.; Ohtsuka, E. X-ray structure of T4 endonuclease V: an excision repair enzyme specific for a pyrimidine dimer. *Science* **1992**, *256*, 523−526.
(21) Vassylyev, D. G.; Kashiwagi, T.; Mikami, Y.; Ariyoshi, M.; Iwai, S.; Ohtsuka, E.; Morikawa, K. Atomic model of a pyrimidine dimer excision repair enzyme complexed with a DNA substrate: Structural basis for damaged DNA recognition. *Cell* **1995**, *83*, 773−782.
(22) Grindley, N. D.; Whiteson, K. L.; Rice, P. A. Mechanisms of site-specific recombination. *Annu. Rev. Biochem.* **2006**, *75*, 567−605.
(23) Guo, F.; Gopaul, D. N.; Van Duyne, G. D. Structure of Cre recombinase complexed with DNA in a site-specific recombination synapse. *Nature* **1997**, *389*, 40−46.
(24) Van Duyne, G. D. A structural view of cre-loxp site-specific recombination. *Annu. Rev. Biophys. Biomol. Struct.* **2001**, *30*, 87−104.
(25) Suzuki, Y.; Endo, M.; Katsuda, Y.; Ou, K.; Hidaka, K.; Sugiyama, H. DNA origami based visualization system for studying site-specific recombination events. *J. Am. Chem. Soc.* **2014**, *136*, 211−218.
(26) Ghosh, K.; Lau, C. K.; Gupta, K.; Van Duyne, G. D. Preferential synapsis of loxP sites drives ordered strand exchange in Cre-loxP site-specific recombination. *Nat. Chem. Biol.* **2005**, *1*, 275−282.
(27) Gopaul, D. N.; Guo, F.; Van Duyne, G. D. Structure of the Holliday junction intermediate in Cre-loxP site-specific recombination. *EMBO J.* **1998**, *17*, 4175−4187.
(28) Endo, M.; Tatsumi, K.; Terushima, K.; Katsuda, Y.; Hidaka, K.; Harada, Y.; Sugiyama, H. Direct visualization of the movement of a single T7 RNA polymerase and transcription on a DNA nanostructure. *Angew. Chem., Int. Ed.* **2012**, *51*, 8778−8782.
(29) Bacolla, A.; Wells, R. D. Non-B DNA conformations, genomic rearrangements, and human disease. *J. Biol. Chem.* **2004**, *279*, 47411−47414.
(30) Bacolla, A.; Wells, R. D. Non-B DNA conformations as determinants of mutagenesis and human disease. *Mol. Carcinog.* **2009**, *48*, 273−285.
(31) Shirude, P. S.; Okumus, B.; Ying, L.; Ha, T.; Balasubramanian, S. Single-molecule conformational analysis of G-quadruplex formation in the promoter DNA duplex of the proto-oncogene c-kit. *J. Am. Chem. Soc.* **2007**, *129*, 7484−7485.
(32) Sannohe, Y.; Endo, M.; Katsuda, Y.; Hidaka, K.; Sugiyama, H. Visualization of dynamic conformational switching of the G-quadruplex in a DNA nanostructure. *J. Am. Chem. Soc.* **2010**, *132*, 16311−16313.
(33) Xu, Y.; Sato, H.; Sannohe, Y.; Shinohara, K.; Sugiyama, H. Stable lariat formation based on a G-quadruplex scaffold. *J. Am. Chem. Soc.* **2008**, *130*, 16470−16471.
(34) Rajendran, A.; Endo, M.; Hidaka, K.; Lan Thao Tran, P.; Mergny, J. L.; Sugiyama, H. Controlling the stoichiometry and strand polarity of a tetramolecular G-quadruplex structure by using a DNA origami frame. *Nucleic Acids Res.* **2013**, *41*, 8738−8747.
(35) Rajendran, A.; Endo, M.; Hidaka, K.; Tran, P. L.; Mergny, J. L.; Gorelick, R. J.; Sugiyama, H. HIV-1 nucleocapsid proteins as molecular chaperones for tetramolecular antiparallel G-quadruplex formation. *J. Am. Chem. Soc.* **2013**, *135*, 18575−18585.
(36) Jungmann, R.; Steinhauer, C.; Scheible, M.; Kuzyk, A.; Tinnefeld, P.; Simmel, F. C. Single-molecule kinetics and super-resolution microscopy by fluorescence imaging of transient binding on DNA origami. *Nano Lett.* **2010**, *10*, 4756−4761.
(37) Asanuma, H.; Liang, X.; Nishioka, H.; Matsunaga, D.; Liu, M.; Komiyama, M. Synthesis of azobenzene-tethered DNA for reversible photo-regulation of DNA functions: hybridization and transcription. *Nat. Protoc.* **2007**, *2*, 203−212.
(38) Liang, X.; Mochizuki, T.; Asanuma, H. A supra-photoswitch involving sandwiched DNA base pairs and azobenzenes for light-driven nanostructures and nanodevices. *Small* **2009**, *5*, 1761−1768.
(39) Endo, M.; Yang, Y.; Suzuki, Y.; Hidaka, K.; Sugiyama, H. Single-molecule visualization of the hybridization and dissociation of photoresponsive oligonucleotides and their reversible switching behavior in a DNA nanostructure. *Angew. Chem., Int. Ed.* **2012**, *51*, 10518−10522.
(40) Jovin, T. M.; Soumpasis, D. M.; Mcintosh, L. P. The transition between B-DNA and Z-DNA. *Annu. Rev. Phys. Chem.* **1987**, *38*, 521−560.
(41) Mao, C. D.; Sun, W. Q.; Shen, Z. Y.; Seeman, N. C. A nanomechanical device based on the B-Z transition of DNA. *Nature* **1999**, *397*, 144−146.
(42) Rajendran, A.; Endo, M.; Hidaka, K.; Sugiyama, H. Direct and real-time observation of rotary movement of a DNA nanomechanical device. *J. Am. Chem. Soc.* **2013**, *135*, 1117−1123.
(43) Behe, M.; Felsenfeld, G. Effects of methylation on a synthetic polynucleotide: the B-Z transition in poly(dG-m5dC).poly(dG-m5dC). *Proc. Natl. Acad. Sci. U.S.A.* **1981**, *78*, 1619−23.
(44) Bath, J.; Turberfield, A. J. DNA nanomachines. *Nat. Nanotechnol.* **2007**, *2*, 275−284.
(45) Wickham, S. F. J.; Endo, M.; Katsuda, Y.; Hidaka, K.; Bath, J.; Sugiyama, H.; Turberfield, A. J. Direct observation of stepwise movement of a synthetic molecular transporter. *Nat. Nanotechnol.* **2011**, *6*, 166−169.
(46) Bath, J.; Green, S. J.; Turberfield, A. J. A free-running DNA motor powered by a nicking enzyme. *Angew. Chem., Int. Ed.* **2005**, *44*, 4358−4361.
(47) Wickham, S. F. J.; Bath, J.; Katsuda, Y.; Endo, M.; Hidaka, K.; Sugiyama, H.; Turberfield, A. J. A DNA-based molecular motor that can navigate a network of tracks. *Nat. Nanotechnol.* **2012**, *7*, 169−173.
(48) Lund, K.; Manzo, A. J.; Dabby, N.; Michelotti, N.; Johnson-Buck, A.; Nangreave, J.; Taylor, S.; Pei, R.; Stojanovic, M. N.; Walter, N. G.; Winfree, E.; Yan, H. Molecular robots guided by prescriptive landscapes. *Nature* **2010**, *465*, 206−210.
(49) Gu, H. Z.; Chao, J.; Xiao, S. J.; Seeman, N. C. A proximity-based programmable DNA nanoscale assembly line. *Nature* **2010**, *465*, 202−205.
(50) Mori, T.; Hirose, A.; Hagiwara, T.; Ohtsuka, M.; Kakuta, Y.; Kimata, K.; Okahata, Y. Single-molecular enzymatic elongation of hyaluronan polymers visualized by high-speed atomic force microscopy. *J. Am. Chem. Soc.* **2012**, *134*, 20254−20257.
(51) Suzuki, Y.; Endo, M.; Yang, Y.; Sugiyama, H. Dynamic assembly/disassembly processes of photoresponsive DNA origami nanostructures directly visualized on a lipid membrane surface. *J. Am. Chem. Soc.* **2014**, *136*, 1714−1717.
(52) Ando, T. High-speed atomic force microscopy coming of age. *Nanotechnology* **2012**, *23*, 062001.
(53) Kodera, N.; Yamamoto, D.; Ishikawa, R.; Ando, T. Video imaging of walking myosin V by high-speed atomic force microscopy. *Nature* **2010**, *468*, 72−76.
(54) Steinhauer, C.; Jungmann, R.; Sobey, T. L.; Simmel, F. C.; Tinnefeld, P. DNA origami as a nanoscopic ruler for super-resolution microscopy. *Angew. Chem., Int. Ed.* **2009**, *48*, 8870−8873.
(55) Gietl, A.; Holzmeister, P.; Grohmann, D.; Tinnefeld, P. DNA origami as biocompatible surface to match single-molecule and ensemble experiments. *Nucleic Acids Res.* **2012**, *40*, e110.
(56) Jungmann, R.; Scheible, M.; Simmel, F. C. Nanoscale imaging in DNA nanotechnology. *Wiley Interdiscip. Rev.: Nanomed. Nanobiotechnol.* **2012**, *4*, 66−81.
(57) Stein, I. H.; Schuller, V.; Bohm, P.; Tinnefeld, P.; Liedl, T. Single-molecule FRET ruler based on rigid DNA origami blocks. *ChemPhysChem* **2011**, *12*, 689−695.

(58) Stein, I. H.; Steinhauer, C.; Tinnefeld, P. Single-molecule four-color FRET visualizes energy-transfer paths on DNA origami. *J. Am. Chem. Soc.* **2011**, *133*, 4193−4195.
(59) Schmied, J. J.; Gietl, A.; Holzmeister, P.; Forthmann, C.; Steinhauer, C.; Dammeyer, T.; Tinnefeld, P. Fluorescence and super-resolution standards based on DNA origami. *Nat. Methods* **2012**, *9*, 1133−1134.